

# Aerodynamic noise simulation of the flow past an airfoil trailing-edge using a hybrid zonal RANS-LES

Fabrice Mathey \*

*Fluent France, 1 Place Charles de Gaulle, 78180 Montigny Le Bretonneux, France*

Received 1 October 2006; received in revised form 18 January 2007; accepted 2 April 2007

Available online 29 September 2007

## Abstract

This paper documents the evaluation of a zonal RANS-LES approach for the prediction of broadband and tonal noise generated by the flow past an airfoil trailing edge at a high Reynolds number. A multi-domain decomposition is considered, where the acoustic sources are resolved with a LES sub-domain embedded in the RANS domain. At the RANS-LES interface, a stochastic vortex method is used to generate synthetic turbulent perturbations. The simulations are performed with the general-purpose unstructured control-volume code FLUENT. The far-field noise is calculated using the aeroacoustic analogy of Ffowcs-Williams and Hawkings. The results of the simulation are compared with available acoustic and mean velocity measurements. The investigation demonstrates the ability of this approach to predict the aerodynamic and aeroacoustic properties of the flow. Two simulations are performed in order to address the sensitivity of the results to the perturbation model. The comparison clearly indicates the critical influence of the model.

© 2007 Elsevier Ltd. All rights reserved.

## 1. Introduction

This study deals with numerical prediction of airfoil trailing edge noise. Trailing-edge aeroacoustics is of importance in both aeronautical and naval applications. The dipole sound produced by the edge scattering of pressure fluctuations at a trailing edge is most often an undesirable effect. These pressure fluctuations are created by turbulent eddies as they are convected over the trailing edge. This causes edge scattering of noise to the far field. This scattering mechanism can produce strong broadband and/or tonal noise which is radiated to the far field.

In this work, an Hybrid zonal RANS/LES unsteady CFD simulation is used to get a prediction of the acoustic sources, which are then used as an entry data of an acoustic propagation model. The case under study corresponds to the recent experiment conducted by Kunze [1]. The trailing edge shape considered is identical with one of the trailing edge shapes previously investigated by Blake [2].

The accurate prediction of such a high Reynolds number flow requires computational resources which are beyond the capabilities of “usual” computers. Previous CFD studies of trailing-edge flow include the use of LES [3] and DES [4] methods. All these approaches showed limitations in solving the overall problem. The primary limitation of LES to practical use is the computational resource necessary to resolve the entire foil geometry with a sufficient spanwise extent. Furthermore it was shown [4] that premature separation can occur with DES due to the statistical loss of upstream turbulence in the transition from RANS to LES. In this paper, a zonal RANS/LES method is considered to perform the numerical predictions of aerodynamic noise sources at a moderate computational cost. The idea is to restrict the expensive LES calculation to the aeroacoustic source regions, while the rest of the configuration can be treated by a much cheaper RANS approach. The sound propagation is handled by a specific numerical tool (a Ffowcs-Williams Hawking acoustic analogies for instance).

Zonal RANS/LES methods are based on a discontinuous treatment between the RANS and LES models whereas other hybrid approaches like DES assume a continuous

\* Tel.: +33 1 30 60 98 97; fax: +33 1 30 64 98 43.

E-mail address: [fabrice.mathey@fluent.fr](mailto:fabrice.mathey@fluent.fr)

treatment between the two models. The advantage of the zonal approach is thus the removing of the so called “gray area” where the behavior of the model is neither RANS nor LES. However in this case it is necessary to account for the discontinuity between the two different descriptions of the turbulence between the RANS and the LES approaches [5–7]. A possible way to implement interface conditions is to consider overlap region between the two models. For instance Quéméré and Sagaut [5] derived a consistent approach for the treatment of the discontinuity at the lateral and outflow boundaries by considering a global RANS domain and a small overlapping region devoted to LES. Extrapolation and averaging technique were considered to provide the appropriate boundary conditions for the LES and RANS domains. Schlutler et al. [7] considered two different flow solvers coupled at the RANS/LES inflow and outflow boundaries. Averaging technique and driving source terms were considered in an overlap region between the LES and RANS domain to treat the discontinuity. These approaches all share a common issue however, namely the definition of appropriate unsteady inflow conditions at the RANS/LES interface where a fully turbulent flow enters the LES region. The conversion of statistically steady modeled turbulence to unsteady resolved turbulence is a complex task which requires further modeling assumption. Several techniques can be considered. For example precursor domains or recycling methods [8], are probably the most accurate techniques that can be considered. Typically, such simulations would need to be run a priori or simultaneously as the main computation that requires specification of turbulence at its inlets. This approach is commonly used for simple geometries but the generalization of such method to arbitrary complex 3D geometries presents some significant challenges. For instance the inlet must be placed in a region where the flow is in an equilibrium state. To circumvent this issue, synthetic inlet boundary conditions have been proposed where the fluctuations are created artificially [9–11]. These methods are usually based on random fluctuations with given moment and spectra superposed to a mean velocity profiles. However compared to recycling method, the synthetic turbulence generated by these methods is usually not a realistic representation of turbulent eddies, and for example do not contain any phase information. Therefore the turbulence is not sustained and long adjustment distances can be required for realistic statistics to be established before the region of interest [11]. The experience base is not sufficient to understand the generality and the accuracy of these methods.

In this paper, an alternative approach is considered. The vortex method [12] is used to generate the turbulent fluctuations at the explicit RANS/LES interface. Extensive validations [12–14] have shown that the VM offers a relative inexpensive and accurate way to generate fluctuations representing a turbulent flow field at the inlet of a LES domain. Because of the assumed shape of eddies, the generated velocity field is temporally and spatially correlated,

and take into account the anisotropy of the flow in the near-wall region. It is thus a much more realistic representation of turbulence than the one obtained with a simple velocity distribution using a random generator. This method was recently implemented as standard boundary conditions for LES simulation in FLUENT [15]. In the current study, the method is adapted for an embedded LES sub-domain inside an RANS domain. Moreover, the influence of the model is addressed in the specific context of acoustic sources prediction.

## 2. Methodology

A multi-domain RANS/LES approach is considered where each domain is solved in either RANS or LES mode. The LES sub-domain is considered to solve accurately the aero-acoustic sources. Non conformal interfaces are considered at the boundaries of the LES domain to match the RANS mesh. At the RANS/LES interfaces where the grid is suddenly refined, the turbulent viscosity model switch from RANS to LES. Although more advanced boundary conditions could be considered [5], the RANS values are directly used at the lateral and outflow boundaries of the LES domain. Similarly, a direct injection of the LES field is considered to create boundary conditions for the RANS domain. However for the inflow boundary of the LES domain, as the modeled RANS Reynolds stress is vanishing, the LES requires the generation of explicitly resolved turbulent eddies. In order to construct these time-dependent inlet conditions, a random 2D vortex method is considered. With this approach, a perturbation is added to the mean velocity via a fluctuating two-dimensional vorticity field (two-dimensional in the plane normal to the streamwise direction). The vortex method is based on the Lagrangian form of the 2D evolution equation of the vorticity:

$$\frac{\partial \omega}{\partial t} + (\vec{u} \cdot \nabla) \omega = \nu \nabla^2 \omega \quad (1)$$

where the velocity vector is decomposed as follow:

$$\vec{u} = \nabla \times \vec{\psi} + \nabla \phi \quad (2)$$

$\psi$  is the 2D stream function and  $\phi$  is the velocity potential. Taking the curl of this equation, one obtains:

$$\omega = -\nabla^2 \psi \quad (3)$$

The solution of (3) is given by the convolution of the vorticity with the 2D Green’s function:

$$\psi(\vec{x}) = -\frac{1}{2\pi} \int_{R^2} \ln |\vec{x} - \vec{x}'| \omega(\vec{x}') d\vec{x}' \quad (4)$$

This relation is used in Eq. (2) to yield the relation commonly known as the Biot Savart law:

$$u(\vec{x}) = -\frac{1}{2\pi} \int_{R^2} \frac{(\vec{x} - \vec{x}') \times \omega(\vec{x}') \cdot \vec{z}}{|\vec{x} - \vec{x}'|^2} d\vec{x}' \quad (5)$$

A particle discretization is used in order to solve Eq. (1). These particles or “vortex points” are convected randomly and carry information about the vorticity field. If  $N$  is the number of vortex points and  $S$  the area of the inlet section, the amount of vorticity carried by a given particle  $i$  is represented by the circulation  $\Gamma_i$ , and an assumed spatial distribution  $\eta$ :

$$\omega(\vec{x}, t) = \sum_{i=1}^N \Gamma_i(t) \eta(|\vec{x} - \vec{x}_i|, t) \quad (6)$$

with

$$\Gamma_i(x) = 4 \sqrt{\frac{\pi S k(x)}{3N(2 \ln(3) - 3 \ln(2))}} \quad (7)$$

$$\eta(x) = \frac{1}{2\pi\sigma^2} \left( 2e^{-\frac{|x|^2}{2\sigma^2}} - 1 \right) e^{-\frac{|x|^2}{2\sigma^2}} \quad (8)$$

where  $k$  is the turbulence kinetic energy and  $\mathbf{x}$  the vector position of the vortex point. Eq. (7) is derived from the turbulent kinetic energy, noting that the intensity of the vortices depends on their circulation. The root mean square velocity fluctuations induced by one vortex in the inlet plane can be approximated by:

$$u_{\text{rms}}^2(\vec{x}) = \frac{1}{S} \int \int_{R^2} u^2(\vec{x}) ds \quad (9)$$

For  $N$  vortices, integration of Eq. (9) over  $S$ , gives:

$$u_{\text{rms}}^2(\vec{x}) = \frac{N\Gamma^2(2 \ln(3) - 3 \ln(2))}{4\pi S} \quad (10)$$

The circulation in Eq. (7) is derived from (10) with an isotropy hypothesis. It should be noted however that this hypothesis is considered only for the fluctuations parallel to the inlet plane. Finally the shape of the vortices in Eq. (8) is given by a modified Gaussian function. The parameter  $\sigma$  provides control over the size of a vortex particle. The resulting discretization for the velocity field is thus given by:

$$\vec{u}(\vec{x}) = \frac{1}{2\pi} \sum_{i=1}^N \Gamma_i \frac{(\vec{x}_i - \vec{x}) \times \vec{z}}{|\vec{x}_i - \vec{x}|^2} \left( 1 - e^{-\frac{|\vec{x}_i - \vec{x}|^2}{2\sigma^2}} \right) e^{-\frac{|\vec{x}_i - \vec{x}|^2}{2\sigma^2}} \quad (11)$$

where the vector  $\mathbf{z}$  in Eq. (11) is the unit vector in the stream-wise direction. Originally [12], the size of the vortex was fixed by an ad hoc value of  $\sigma$ . In order to make this method generally applicable, a local vortex size is specified through a turbulent mixing length hypothesis. Consequently,  $\sigma$  is calculated from the known profiles of mean turbulence kinetic energy and mean dissipation rate at the inlet according to:

$$2\sigma = ck^{3/2}/\varepsilon \quad (12)$$

where  $c = C_\mu^{3/4}$ . In order to ensure that the vortex always belongs to the resolved scales, the minimum value of  $\sigma$  in Eq. (12) is bounded by the local grid size. The sign of the circulation of each vortex is changed randomly after a characteristic turbulent time scale  $\tau = \kappa/\varepsilon$  has passed. In

the present work, a simplified linear kinematic model is considered for the stream wise velocity fluctuations. This model mimics the influence of the 2D vortex on the stream-wise mean velocity field. If the mean stream-wise velocity  $U$  is considered as a passive scalar, the fluctuation  $u'$  resulting from the transport of  $U$  by  $\mathbf{v}'$  (where  $\mathbf{v}'$  is the planar fluctuating 2D velocity field as computed by the VM) can be modelled by  $u' = -\mathbf{v}' \cdot \mathbf{g}$  where  $\mathbf{g}$  is the unit vector aligned with the mean inlet velocity gradient. When this mean velocity gradient is equal to zero, a random perturbation can be considered instead.

Virtual body forces are employed in the momentum equations to add the reconstructed turbulent fluctuations to the velocity field. The source term reads:

$$(U_n + u'_n) \cdot \vec{u}' \cdot S_n + (u'_n) \cdot \vec{U} \cdot S_n \quad (13)$$

where  $U_n = \mathbf{U} \cdot \mathbf{n}$ ,  $u'_n = \mathbf{u}' \cdot \mathbf{n}$  and  $\mathbf{n}$  denotes the unit vector normal to the RANS/LES interface  $S_n$ . These virtual body forces are considered only in the first LES cells close to the RANS/LES interfaces. These virtual body forces and the zonal RANS/LES turbulent eddy viscosity model are implemented in FLUENT via User Define Functions [15]. The RANS-SST [16] model is used in the RANS region and the WALE [17] model is considered in the refined LES grid region.

All calculations reported in this paper have been obtained using the compressible formulation of FLUENT V6.3 general-purpose control-volume code. FLUENT employs a cell-centered finite-volume method based on a multi-dimensional linear reconstruction scheme, which permits use of computational elements with arbitrary topology. In the present study, only hexahedral cells were considered. For the computations presented in this paper, the segregated solver of FLUENT was used. With this solver, the governing equations are solved sequentially. The temporal discretization employs a fully-implicit, three-level second-order scheme. The Fractional step method [18] is considered for the pressure-velocity coupling. Convective and diffusive fluxes are discretized using second-order central differencing. The discretized algebraic equations are solved using a point-wise Gauss-Seidel iterative algorithm. An algebraic multi-grid (AMG) method is employed to accelerate solution convergence. Finally the solver is fully parallelized. More details about the finite-volume method can be found in Mathur and Murthy [19] and Kim [20].

### 3. Test case

A low turbulence free-jet wind tunnel with a test section of 0.61 by 0.61 is fitted into an anechoic chamber. A flat airfoil with an elliptical leading edge and an asymmetric 45° rounded trailing edge is placed in the test section. Half of the model extends into the inlet section of the wind tunnel. The trailing edge shape is identical with one of the trailing edge shapes investigated by Blake [2]. The elliptical leading edge was chosen to prevent flow separation. The

chord length of the model is 0.91 m with a maximum thickness of 0.05 m and a width of 0.61 m. The Reynolds number based on the free-stream velocity  $U_{inf} = 30.5$  m/s and the chord is  $1.8 \times 10^6$ . In the experiment, the boundary layer thickness is measured equal to 0.01 m on the suction side prior to the beginning of the curvature of the model. This corresponds also to the location of the RANS/LES interface. Two microphones are attached to a boom and are placed at 1.83 m away from the trailing edge. The computational domain is decomposed into a quasi 2D laminar sub-domain, a quasi 2D turbulent RANS sub-domain and a non-conformal LES sub-domain embedded inside the RANS domain, as shown in Fig. 1. The “laminar zone” corresponds to the inlet part of computational domain, including 25% of the airfoil chord length from the leading edge. In this region, both the turbulent production and the turbulent eddy viscosity of the RANS model are set equal to zero. This approach is considered in order to predict the correct growth of the laminar boundary layer prior to the transition location, as in the experiment the transition is triggered at 25% of the chord length on both sides of the model. As shown in Fig. 1, the inlet section of the wind channel is also represented by the simulation.

The grid used for the simulation is shown in Fig. 2. The total number of grid points is nearly equal to  $2 \times 10^6$ , the LES part corresponding to  $1.86 \times 10^6$ . The spanwise extent

of the computational domain is equal to 20% of the chord length. It is assumed that the fluctuating field is periodic in the spanwise direction. In the LES sub-domain, the mesh is stretched in the streamwise and wall normal directions, and is uniform in the spanwise direction. The corresponding LES grid size is  $155 \times 120 \times 100$ . The number of cells used in the spanwise direction of the RANS zone is equal to only four cells, as shown in Fig. 2. In the LES region where the boundary layer remains attached along the airfoil prior to separation, the wall resolution in wall units is  $\Delta x^+ \sim 200, y^+ < 2$  and  $\Delta z^+ \sim 100$  in the wall-normal, streamwise and spanwise directions, respectively. The mesh resolution in the RANS region is also  $y^+ < 2$  in the wall normal direction, but the mesh is coarsened in the other directions.

Two different simulations (hereafter referred as to as RUN1 and RUN2) are performed. The first simulation RUN1 is performed with a random forcing (white noise) at the RANS/LES interface. The random noise is considered here in order to address the sensitivity of the results to the accuracy of the turbulent forcing. White noise is known to produce poor results due to the non-correlated nature of the signal. On the contrary, the perturbation generated by the vortex method is temporally and spatially correlated. This is an important requirement to ensure that the synthetic turbulent field can be sustained. The second

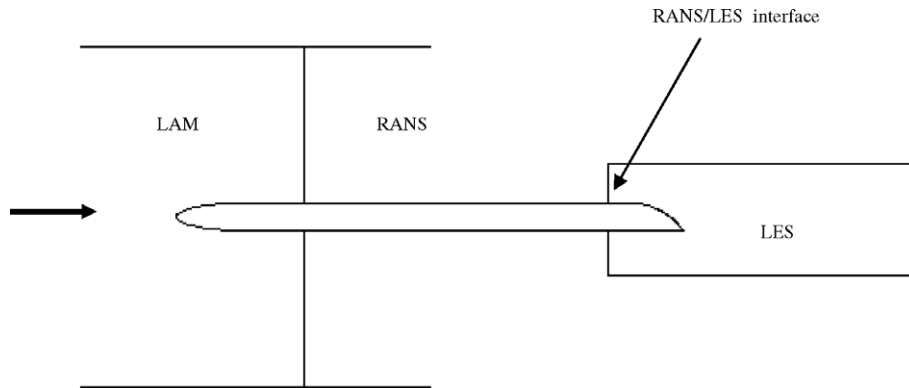


Fig. 1. Sketch of the computational domain and RANS & LES sub-domains.

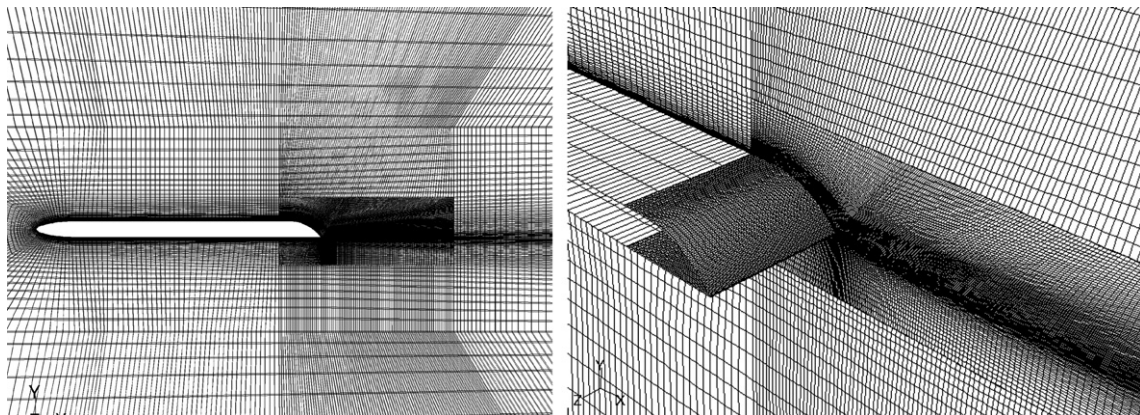


Fig. 2. 2D slice of the computational grid with the embedded LES refined grid.

simulation RUN2 is performed with this vortex method. The time step of both simulation is  $\Delta t = 2 \times 10^{-5}$  s, corresponding to a maximum CFL number less than unity in the trailing edge and near wake region of the flow.

## 4. Results and discussion

### 4.1. Aerodynamic simulation

A qualitative overview of the flow is given in Fig. 3 for the two RANS/LES simulations. Both cases show the fully-developed 3D flow. The upper boundary layer separates gradually in the adverse pressure gradient created by the rounded edge, while the lower boundary layer separates instantly at the sharp edge. The vorticity shed into the flow from the boundary layers is convected downstream creating a Von Karman street. The main shedding can be recognized by oscillations in the wake of the blade. These oscillations are much more pronounced for the simulation without the turbulent forcing. The effect of the turbulent forcing on the instantaneous flow is also visible in Fig. 3. The streamwise turbulent eddies generated at the RANS/LES interface are convected downstream and delay the separation of the boundary layer. These eddies interact with the two dimensional coherent structures generated past the separation points. This interaction results in an early transition of the separated shear layer to a fully 3D state. The topology of the flow simulated by RUN2 is also influenced by these interactions, with more apparent small scales and horse-shoe structures close to the trailing edge.

The mean streamlines of the flow above and in the wake of the trailing edge are compared in Fig. 4. RUN1 predicts a slightly larger separated region and size of the vortices.

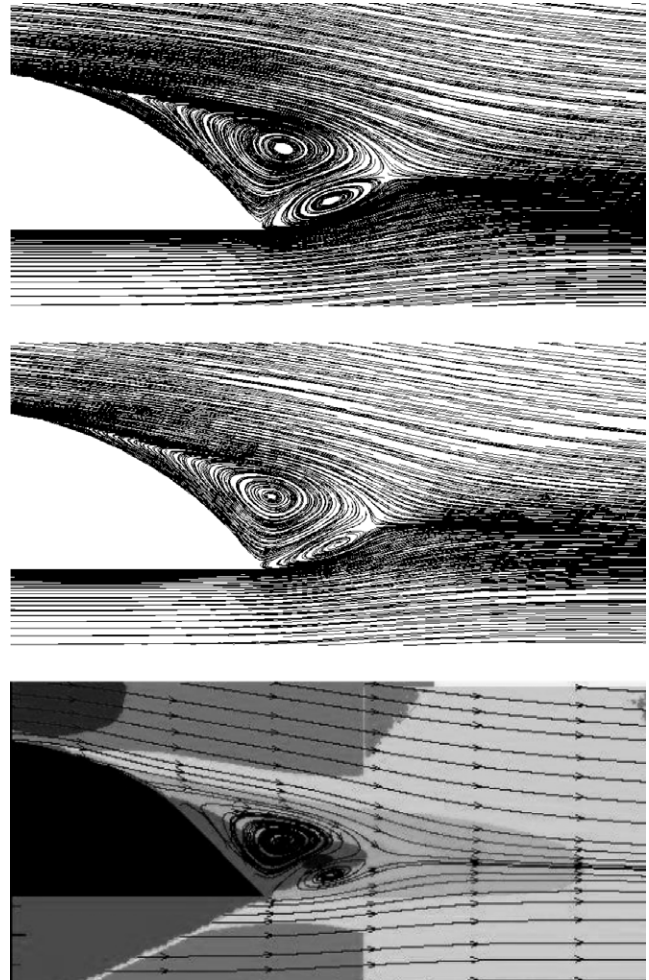


Fig. 4. Mean streamlines of the flow. (a) From top to bottom: RUN1, RUN2 and experiment from Shannon and Morris [16].

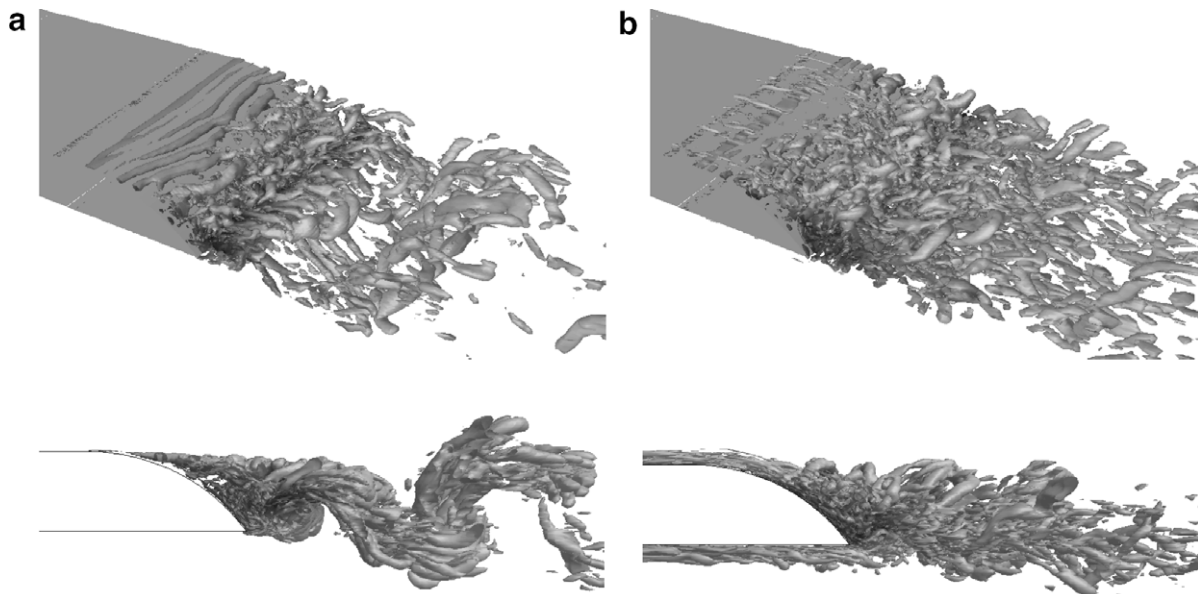


Fig. 3. Visualization of the  $Q$ -criterion in the wake of the airfoil. Isosurface  $Q = 500 \times 105$  colored by the streamwise velocity: a) RUN1 b) RUN2.

RUN2 predicts a narrower wake compared to RUN1. A good resemblance is achieved between RUN2 and the experimental results from Shannon and Morris [23].

The position of the mean separation points are compared in Table 1. RUN2 predicts a separation points which is in better agreement with the experimental data, whereas in RUN1 the separation is predicted farther upstream.

Time-averaged mean streamwise velocity profiles and streamwise rms fluctuations in the wake are given in

Table 1  
Distance (on the  $x$ -axis) of the upper boundary layer separation point from the trailing edge

Simulation	Distance (mm)
RUN1	75
RUN2	55
EXP	45

Fig. 5. Both quantities are reasonably well predicted by RUN2. The velocity deficits are slightly over-predicted in the far wake, and the rms-values are slightly over-predicted on the upper boundary layer side. This could be explained by a slow recovery of the turbulent fluctuations from the synthetic LES inlet. More investigations regarding the sensitivity of the results to the upstream location of the RANS/LES interface would be necessary to address this issue. However RUN1 considerably under-predicts the mean velocity profiles deficit already in the near wake, and considerably over-predicts the velocity fluctuations. This is due to the too rapid decay of the turbulent fluctuations generated by the uncorrelated random noise which is used in RUN1. Both profiles are also shifted to upper boundary layer side, as a result of the early separation of the upper boundary layer predicted by RUN1 (see Fig. 6).

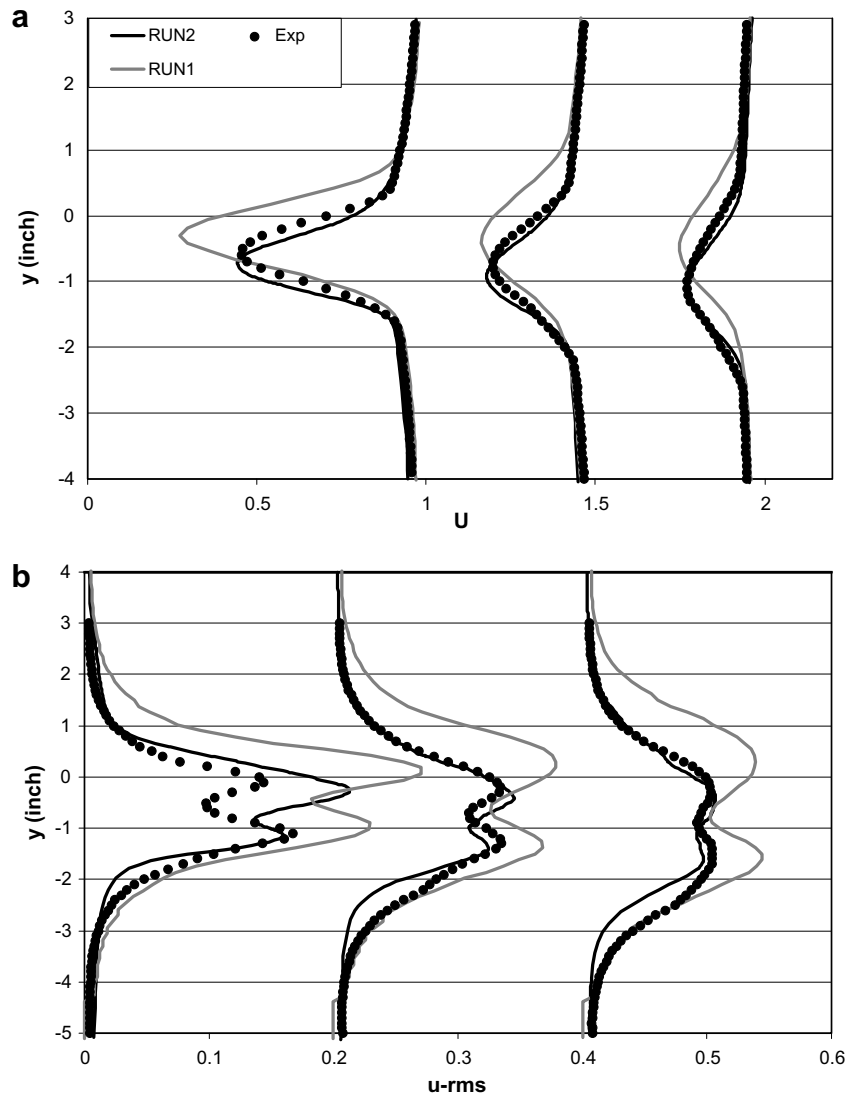


Fig. 5. Comparison of mean streamwise velocity and mean streamwise rms velocity in the wake for  $x = 20$  in.,  $x = 22$  in. and  $x = 24$  in. Measurements from Kunze [1].

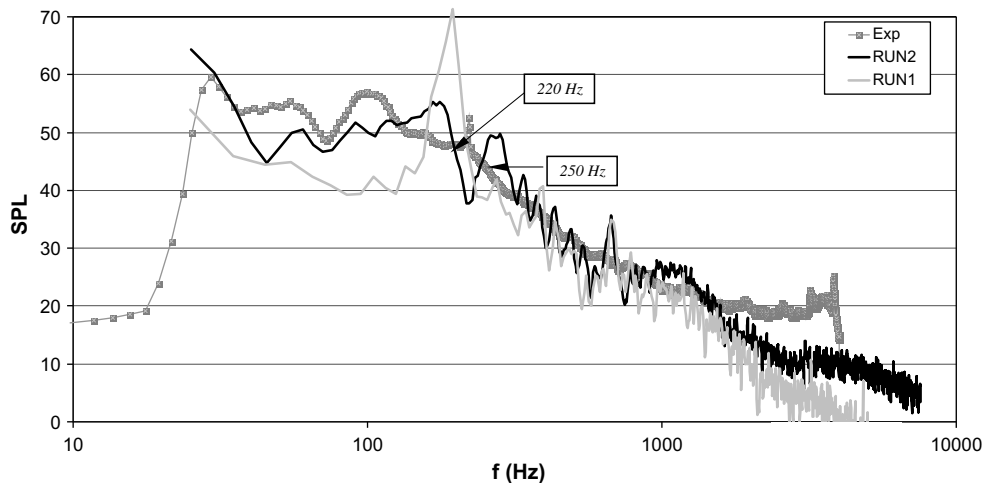


Fig. 6. Comparison of the SPL of the far-field radiated sound for an observer located at a normal distance of 1.83 m from the trailing edge. Measurements from Kunze [1].

#### 4.2. Aeroacoustic prediction

Based on the work of Ffowcs-Williams and Hawkings [21], the far-field noise is calculated by applying the aeroacoustic analogy to the rigid wall surface of the airfoil as the integration surface. The spectra presented above are obtained by a FFT with a length of 10,000 points with 10 averaging and the use of Hanning-window. The simulated span  $L_s = 0.2c$  being less than the span of the test configuration  $L_{exp} = 0.67c$ , a level correction is applied to the simulated spectra [22]. The correlation length of the simulation based on wall pressure coherence at the trailing edge is around  $L = 1c$ , which gives a level correction of 3 dB.

Fig. 5 shows the RANS/LES results in comparison with measurements. The simulation using the VM (RUN2) is in a general good agreement with the broadband spectrum based on the measurements. It should be noted that the background noise of the wind tunnel is still embedded in the experimental signal. At the lower frequency range, the simulation reproduces a main broadband peak also visible in the experiment, although the simulated frequency is over-predicted. The origin of this broadband peak is not explained by Kunze [1] but might be an outcome of the free jet instability which develops from the inlet section and interact downstream with the unsteady wake of the airfoil. The simulation gives further insight into this mechanism. Indeed such instability can be observed in the flow field in Fig. 7.

The tonal peak (at 220 Hz) is also predicted by the simulation, although RUN2 over-predicts the frequency (250 Hz). It is particularly noteworthy that the simulation performed with the white noise (RUN1) over-predicts the amplitude of the tonal peak, and under-predicts its frequency. The broadband noise is also more accurately predicted by RUN2, while RUN1 under-predicts the level both at the low and high frequency range. Finally both simulations predict another tonal peak at higher frequency around  $f = 1000$  Hz. Such tonal frequency might be linked

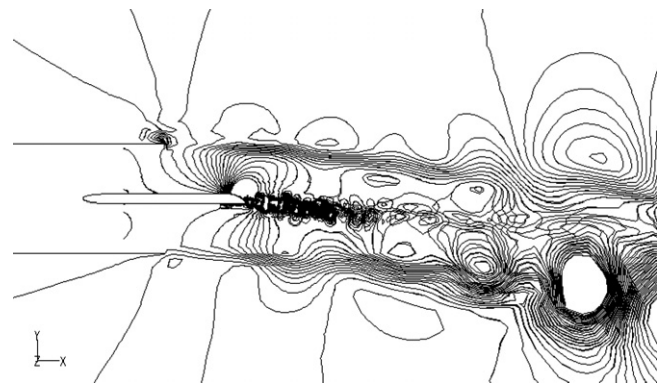


Fig. 7. Contours of the instantaneous vertical velocity  $V_y$ .

to Kelvin-Helmoltz instabilities at the separated boundary layers.

It was shown by Shannon and Morris [23] that the tonal noise results from the large scale coherent structures generated at the separation points. The unsteady surface pressure generated on the surface by these motions is responsible for the acoustic scattering which produces the tonal noise at the vortex shedding frequency. In simulation RUN2, the VM synthetic turbulent perturbation delays the separation point compared to RUN1. This results in a narrower wake as shown by the visualization of the flow and the mean velocity profiles, and explains the increase of the vortex shedding frequency. Finally, interaction between the generated synthetic turbulence and the detached eddies which enhances the mixing and the transition to a fully three-dimensional state may explain the relative damping of the tonal noise and general higher level of broadband noise.

#### 5. Conclusion and future Work

In this work a zonal RANS-LES technique was evaluated to perform the simulation of aeroacoustic trailing edge

noise. A synthetic turbulence generator was considered at the RANS/LES interface and compared to a simple random noise generator. The results showed that this technique is able to capture the separated flow and can reproduce the main characteristics of the aero-acoustics source. Flow statistics indicated that with the random noise generator, a premature separation can exist as turbulence is lost in the transition from RANS to LES. Turbulent fluctuations in the separated zone and in the wake are over-predicted, and the acoustic signature of the trailing edge is not correctly predicted. In particular, the amplitude of the tonal peak frequency corresponding to the Von Karman instability in the wake is overestimated by several decibels. The use of the vortex method to generate the turbulence fluctuations at the inlet of the LES domain improved significantly the accuracy of the simulation. Separation is delayed and the flow statistics in the wake are better predicted. The shape of the acoustics spectrum follows more closely the experimental results. This is an outcome of the turbulence forcing at the LES inlet. The vortex method generates a synthetic turbulent flow field which is spatially correlated. Turbulence is sustained and the turbulent flow recovers more rapidly a three-dimensional state. Therefore the boundary layer separation is delayed and the wake becomes narrow. Interactions in the wake with upstream turbulence damp the strong two-dimensional instability and trigger three-dimensional modes. As a result, the amplitude of the acoustic tonal peak is decreased and more broadband noise can be seen in the spectrum, in better agreement with the experimental results.

Finally it is noted that this high Reynolds number flow was simulated at an affordable cost with the zonal approach. For instance, typical CPU (elapsed time) used for 0.4 s of simulation was approximately 200 h on a opteron (2.2 Ghz) dual-cpu dual-core work-station.

Future work will focus on improvement of the aero-acoustic simulation through implementation of non-reflecting boundary conditions at the boundary of the LES domain. In addition, it is recognized that grid-resolution studies and sensitivity studies of the results to the synthetic generator parameters are necessary to address further the potential of the approach.

### Acknowledgements

Special thanks to Claudia Kunze, University of Notre Dame, Indiana, for providing the author with details of the experimental data. The author is grateful to Davor Cokljat and Sun-Eung Kim, Fluent Inc., for their helpful comments during this work.

### References

- [1] Kunze C. Acoustic and velocity measurements in the flow past an airfoil trailing edge. Master Thesis. University of Notre Dame; 2004.
- [2] Blake WK. A statistical description of pressure and velocity fields at the trailing edge of a flat strut. Technical Report 4241. David W. Taylor Naval Research Center; 1975.
- [3] Wang M, Moin P. Computation of trailing-edge flow and noise using large-eddy simulation. *AIAA J* 2000;38(12):2201–9.
- [4] Paterson EG, Peltier LJ. Detached-Eddy simulation of high Reynolds number beveled-trailing-edge flows and wakes. In: Proceedings of ASME heat transfer/fluids engineering summer conference. Charlotte, North Carolina; July 11–15, 2004.
- [5] Quéméré P, Sagaut P. Zonal multidomain RANS/LES simulations of turbulent flows. *Int J Numer Meth Fluid* 2002;40:903–25.
- [6] Labourasse Sagaut P. Reconstruction of turbulent fluctuations using a hybrid RANS/LES approach. *J Comput Phys* 2002;182(1):301–36.
- [7] Schlüter JU, Pitsh H, Moin P. LES inflow conditions for coupling with Reynolds-averaged flow solvers. *AIAA J* 2003;42(3):478–84.
- [8] Lund TS, Wu X, Squires KD. Generation of turbulent inflow data for spatially-developing boundary layer simulations. *J Comput Phys* 1998;140:233–58.
- [9] Le H, Moin P, Kim J. Direct numerical simulation of turbulent flow over a backward-facing step. *J Fluid Mech* 1997;330:349–74.
- [10] Smirnov A, Shi S, Celik I. Random flow generation technique for large eddy simulation and particle-dynamics modeling. *J Fluids Eng* 123:359.
- [11] Keating A, Piomelli U, Balaras E. A priori and a posteriori tests of inflow conditions for large-eddy simulation. *Phys Fluid* 2004;16(12):4696–712.
- [12] Sergent E. PhD Thesis. L'Ecole Centrale de Lyon, 2004.
- [13] Mathey F, Cokljat D, Bertoglio JP, Sergent E. Assessment of the vortex method for large eddy simulation inlet conditions. *Progress in Computational Fluid Dynamics* 2006;6(1/2/3):58–67.
- [14] Benhamadouche S, Jarrin N, Addad Y, Laurence D. Synthetic turbulent inflow conditions based on a vortex method for large-eddy simulation. *Progr Comput Fluid Dynam* 2006;6(1/2/3):50–7.
- [15] Fluent 6 User's Guide. Fluent Inc., Lebanon NH03766, USA, 2000.
- [16] Menter FR. Two-equation eddy-viscosity turbulence models for engineering applications. *AIAA J* 1994;32(8):1598–605.
- [17] Nicoud F, Ducros F. Subgrid-scale stress modeling based on the square of the velocity gradient tensor. *Flow, Turbul Combust* 1999;62:183–200.
- [18] Kim J, Moin P. Application of a fractional step method to incompressible Navier-Stokes equations. *J Comp Phys* 1985;59:308.
- [19] Kim SE, Mathur SR, Murthy JY, Choudhury D. A Reynolds averaged Navier-Stokes solver using unstructured mesh-based finite-volume scheme. *AIAA-Paper*; 1998. p. 98–0231.
- [20] Kim S. Large eddy simulation using an unstructured mesh based finite-volume solver. *AIAA-Paper-2004-2548*; 2004.
- [21] Ffowcs Williams J, Hawkings D. Sound generated by turbulence and surfaces in arbitrary motion. *Philos Trans Roy Soc* 1969;A264:321–42.
- [22] Kato C, Lida A, Fujita H, Ikegawa M. Numerical prediction of aerodynamic noise from low Mach number turbulent Wake. *AIAA Paper* 1993-0145; 1993.
- [23] Shannon DW, Morris CS. Visualization of blunt trailing edge turbulence. In: Proceedings of the 11<sup>th</sup> international symposium on flow visualization. University of Notre Dame; August 2005.